Electro-assisted adsorption of heavy metals from aqueous solutions by biochar

Zainab Mahdi, Ali El Hanandeh and Qiming Jimmy Yu

ABSTRACT

Electro-assisted adsorption was investigated for Pb^{2+}, Cu^{2+} and Ni^{2+} removal using date seed biochar (DSB-Electro). Compared with pristine biochar, the results showed that DSB-Electro effectively increased the adsorption capacity of Pb^{2+}, Cu^{2+} and Ni^{2+} by 21% to 94%. Significant differences were observed between Pb^{2+} and Cu^{2+} adsorption compared with Ni^{2+}, which could be explained based on ion polarizing power. Under the same voltage, Ni^{2+} solution shows the highest electric conductivity; thereby more Ni^{2+} is transported to the biochar anode, giving them a greater chance to interact with the surface groups. Electro-assisted adsorption occurred rapidly as around 88% of Pb^{2+} and Ni^{2+} adsorbed within the first 3 h, while 96% of Cu^{2+} occurred within the first hour of contact. Reversing the polarity did not seem to cause significant desorption of the adsorbed ions as the amount released from reversing polarity was less than 38%, indicating that only a small fraction of the ions was held by the electrostatic charge introduced by the current. It was likely that the enhanced charge facilitated other adsorption mechanisms by bringing the ions in contact with the biochar initially via electrostatic force. Electro-assisted adsorption can improve the biochar economic feasibility for metals removal (particularly Ni^{2+}) from industrial streams.

Key words | adsorption, date seed biochar, electro-assisted, heavy metal, surface functionality

Zainab Mahdi (corresponding author)
Ali El Hanandeh
Qiming Jimmy Yu
School of Engineering and Built Environment,
Nathan campus,
Griffith University,
Nathan, QLD 4111,
Australia
E-mail: *zainab.mahdi@griffithuni.edu.au*

INTRODUCTION

Heavy metals cause serious environmental and health problems due to their toxic and nonbiodegradable nature. Lead, copper and nickel are among the most commonly used metals. They are classified as toxic and carcinogenic heavy metals (Kaewsarn 2000). Adsorption is known as an effective treatment method for heavy metal removal from contaminated aqueous solutions. Among various adsorbents, activated carbon (AC) is widely used for heavy metal adsorption. However, its high cost may impede its utilization (Ahmad *et al.* 2011). Other more novel adsorbents may also be uneconomical for large-scale applications and may require extensive use of chemicals to manufacture, which may result in higher cost and adverse environmental impacts. Therefore, it is important to develop greener low-cost effective adsorbents.

Biochar is a promising green material that has been utilized successfully to remove contaminants such as heavy metal ions from wastewaters and aqueous solutions (Mohan *et al.* 2014). Biochar is prepared using pyrolysis without further chemical or physical activation. As a result, biochar in its pristine state may have a lower adsorption capacity for heavy metals than AC. Therefore, biochar might require further enhancement to promote its adsorption properties (Rajapaksha *et al.* 2016). Biochar modification to enhance its functionality and adsorption capacity is an emerging field of study.

Several modification methods have been used for biochar modifications including, but not limited to, base and/or acid treatment, steam activation, magnetic modification, and impregnation with minerals. For example, surface modification of the biochar by a feasible chemical process like acid treatment further enhances its adsorption capacity by incorporating highly active –COOH, C = O, C–O, phenolic and alcoholic –OH functional groups on the biochar surface (Sarkar *et al.* 2019). However, most of the modification methods are complicated, time-consuming and require high chemical use. For instance, Sarkar *et al.* (2019) prepared surface modified biochar using high concentration (8 M) of H_2SO_4 with 6 h reaction time. In the study of Wu *et al.* (2017), chemically modified biochars were

doi: 10.2166/wst.2020.163

prepared by mixing the raw biochar with a 1:10 (w/v) ratio of (a) 5% ammonia (NH_3) solution at 50 °C for 9 h; (b) 5% hydrogen peroxide (H_2O_2) solution at 25 °C for 8 h; and (c) 2 M nitric acid (HNO_3) shaken in a reciprocating shaker for 8 h. Furthermore, a special caution must be taken to minimize the effect of modification on the stability of biochar and to avoid the environmental contamination resulting from the modification processes (Rajapaksha *et al.* 2016).

Thus, a simple approach to upgrading the biochar properties and simultaneously enhancing its removal efficiency with simple operation that is less labour intensive in shorter time requirements is favourable. Mahdi *et al.* (2019) demonstrated in laboratory-scale experiments that modification with mild acid (1 M HCl) for 2 h can improve the adsorption capacity of biochar by 27%, 66% and 98% for Pb^{2+}, Cu^{2+} and Ni^{2+} respectively. Nevertheless, it is desirable to eliminate the chemical upgrading process.

Biochar is a highly stable porous carbonaceous material (Chen *et al.* 2011; Ahmad *et al.* 2012), with high surface area (up to 500 $m^2\,g^{-1}$) and high conductivity (up to 4.27 mS cm^{-1}) (Usman *et al.* 2015). It has similar characteristics to AC. Grimm *et al.* (1998) reported that electro-adsorption of AC was best for the removal of several kinds of contaminants and reported an enhancement in its adsorption capacity. Electro-adsorption is a kind of surface adsorption induced by electrical charges generated at low bias potential (Pirkarami *et al.* 2013).

Ying *et al.* (2002) reported that electro-adsorption showed promising results for the heavy metal removal and desalination of dilute solutions. Haro *et al.* (2011) used a porous carbon gel electrode for the electro-assisted removal of ions from brackish water. They compared removal efficiency of the carbon gel electrode with the removal efficiency of AC and AC cloth. They found that the carbon gel showed a better electrochemical performance than AC and carbon cloth, both in terms of ionic removal efficiency, fast electro-adsorption kinetics and regenerability.

Thus, few attempts have recently showed that biochar can be used to prepare a renewable electrode with a reliable adsorption capacity (Jung *et al.* 2015; Stephanie 2017). For instance, Jung *et al.* (2015) fabricated chemically modified biochar derived from marine macroalgae by applying $MgCl_2$ as an electrolyte in an aluminium-electrode based electro-modification system. They suggested that electro-assisted adsorption can offer dual advantages by reducing preparation time and simultaneously enhancing the biochar physiochemical characteristics, resulting in significant adsorption uptake.

Unlike other conventional technologies such as ion exchange, evaporation, reverse osmosis and electrodialysis, electro-adsorption offers several advantages. Ying *et al.* (2002) and Zou *et al.* (2008) reported that electro-assisted adsorption provides several advantages by eliminating the need to use acids, bases, or salt solutions, thereby substantially reducing the amount of any potential secondary waste. Unlike the evaporation process, electro-adsorption consumes less energy to achieve similar results as well as having operational advantages over electrodialysis and reverse osmosis because no membranes are required (Ying *et al.* 2002).

Hence, such recent advances in the electro-assisted adsorption process have motivated the present study and make it possible to develop an innovative method for high adsorption of heavy metal removal onto biochar. The aim of this study is to develop an effective green adsorbent for heavy metal removal. This includes: (1) develop a simple and effective method for the preparation of biochar without using harsh chemicals (greener process) to enhance its heavy metal adsorptive capacity; (2) assess the heavy metal removal ability of the biochars (electro-assisted) including an elaborative adsorption isotherm and kinetic studies; and (3) identify the interaction mechanisms governing the adsorption of heavy metal ions onto electro-assisted biochar adsorbents.

MATERIALS AND METHODS

Chemicals

All chemicals used in the experimental work were of analytical grade. Stock solutions of 5.0 mM of Cu^{2+}, Pb^{2+} and Ni^{2+} were prepared by dissolving a specific quantity of each metal salt ($Pb(NO_3)_2$, $Cu(NO_3)_2$ $2.5H_2O$, and $Ni(NO_3)_2$ $6H_2O$) in 1.0 L deionized water. Then for adsorption experiments, working metal solutions of 0.3, 0.5, 1.0, 1.5, 3.0, 3.5 and 4.0 mM were prepared by diluting with deionized water to the required concentrations. The diluted solutions and standard solutions for atomic absorption spectroscopy (AAS) analysis were freshly prepared before use and discarded after use. Deionized water was used in all chemical solution preparation and adsorption experiments. All the prepared solutions were stored in acid-washed glass containers at room temperature for further use.

Biochar preparation

The biochar preparation followed the procedure described in our earlier work (Mahdi *et al.* 2019). Briefly, date seed

biomass was collected after physical separation of the date flesh fruit. The seeds were washed several times with deionized water and then oven dried for 2 days at 50 °C before it was pyrolysed at 550 °C for 3 h. The resultant biochar was gently crushed and sieved to a particle size range of 0.6–1.4 mm. Biochar samples were washed with deionized water to remove fine particles and soluble salts. Then, the biochar samples were oven-dried at 105 °C for 2 h and stored in airtight containers. The pristine biochar was labelled according to its pyrolysis temperature and time as DSB550-3.

Electro-assisted adsorption of biochar

The electro-adsorption experiment was performed with a two-electrode configuration in a beaker cell. The schematic set-up for electro-adsorption is shown in Figure S1 (see Supplementary Material). For the electro-adsorption experiment, 1.0 g of the pristine biochar was formed as a working electrode (DSB-Electro). The biochar was placed inside a permeable tube and connected by electrical wire. For the reference electrode (anode), a piece of electrical copper wire was also used. Both electrical wires were attached to a DC power supply (GBC-30300G) to provide a constant voltage: 0.1 V for Pb^{2+} and 0.2 V for both Cu^{2+} and Ni^{2+} to ensure that the metal ion was not oxidized or reduced during the electro-adsorption process and also that the reference electrode would not be ionized. The beaker cell was filled with the metal solution and the initial pH of the solution was adjusted to the required pH value of 6.0 using 0.1 M HCl and NaOH solutions. The beaker was kept for 24 h to achieve equilibrium under an electrical field. Then, 1 mL samples were withdrawn at predetermined time intervals and the metal concentration was determined using AAS (Avanta-GBC, USA) with an air–acetylene flame.

Batch adsorption experiments were run at room temperature (23 ± 2 °C) by mixing 0.1 g of each biochar sample in 10 mL of working solutions of Pb^{2+}, Cu^{2+} and Ni^{2+}. At the start of the experiment, initial pH was adjusted to pH 6.0 ± 0.1 using 0.1 M NaOH or HCl solutions. The solution was filtered using pre-cleaned glass syringe combined with 0.45 μm Millipore filters and the samples were analysed using AAS. The adsorption capacity of each metal ion adsorbed by the biochar was determined (q_e, mmol g^{-1}) as the difference between the initial and final concentrations as given in Equation (1):

$$q_e = \frac{(C_o - C_e)V}{W} \tag{1}$$

where C_o is initial metal concentration (mM), C_e metal concentration at equilibrium (mM), V is volume of metal solution (L), and W is amount of biochar (g). All adsorption experiments were conducted in triplicate and the average values and the standard error were used to express the error bar. To establish a reference for comparison, adsorption kinetics and isotherm experiments were also conducted without electro-assistance under the same laboratory conditions.

Modelling of adsorption equilibrium and kinetics

The relationship between the amounts of metal adsorbed (q_e, mmol g^{-1}) and metal concentrations (C_e, mM) at equilibrium were modelled using Langmuir, Freundlich and Sips isotherms. The Langmuir equation can be expressed as in Equation (2)

$$q_e = \frac{q_m K_L C_e}{1 + K_L C_e} \tag{2}$$

where K_L is the adsorption constant (L $mmol^{-1}$) related to energy of adsorption, q_m is the maximum adsorption capacity (mmol g^{-1}) and C_e metal concentration at equilibrium (mM).

The non-linear form of Freundlich equation is written as Equation (3):

$$q_e = K_F C_e^{\frac{1}{n}} \tag{3}$$

where K_F and n are Freundlich constants indicating the adsorption capacity and the adsorption intensity, respectively.

Sips isotherm, combination of Langmuir and Freundlich isotherms, is used for predicting the heterogeneous adsorption systems. When the metal concentrations are low, Sips effectively reduces to the Freundlich isotherm while at high metal concentrations, it approaches the Langmuir isotherm and it is written as given in Equation (4):

$$q_e = \frac{K_S C_e^{\beta_S}}{1 + a_S C_e^{\beta_S}} \tag{4}$$

where K_S is the Sips model isotherm constant (L g^{-1}), a_S the Sips model constant (L $mmol^{-1}$) and β_S the Sips model exponent.

Several models exist to describe the adsorption kinetics and rate-limiting step; the pseudo first and pseudo second

order rate models are the most popular. Pseudo first order rate model can be expressed as in Equation (5):

$$q_t = q_e(1 - e^{-k_1 t}) \tag{5}$$

where q_t is the amount of metal ion adsorbed per unit mass (mmol g^{-1}) at time t and k_1 (min^{-1}) is the pseudo first order adsorption rate constant.

Non-linear form of pseudo second order model is expressed by Equation (6):

$$q_t = \frac{q_e^2 k_2 t}{1 + q_e k_2 t} \tag{6}$$

where k_2 is the equilibrium rate constant of pseudo second order adsorption (g (mmol min)$^{-1}$).

All parameters for the isotherm and kinetics models were obtained using the regression tool in MATLAB™.

RESULTS AND DISCUSSION

Equilibrium isotherms

Adsorption isotherms of Pb^{2+}, Cu^{2+} and Ni^{2+} on the biochar without electro-assisted (DSB550-3) and with electro-assisted biochar (DSB-Electro) are shown in Figures 1–3. As shown from the figures the equilibrium adsorption uptakes of the electro-assisted biochar to the heavy metals were higher than that of the DSB550-3. The adsorption capacity (q_{max} mmol g^{-1}) of DSB-Electro biochar was determined to be 0.867, 0.572 and 0.646, which is significantly higher than that of the DSB550-3 (0.718, 0.421 and 0.333) for Pb^{2+}, Cu^{2+} and Ni^{2+}, respectively. The lowest improvement (21% increase) was observed in the case of Pb^{2+} while the best improvement was observed in the case of Ni^{2+} (94%). Han *et al.* (2006) found that the enhancement of adsorption capacity for the adsorbate onto the adsorbent

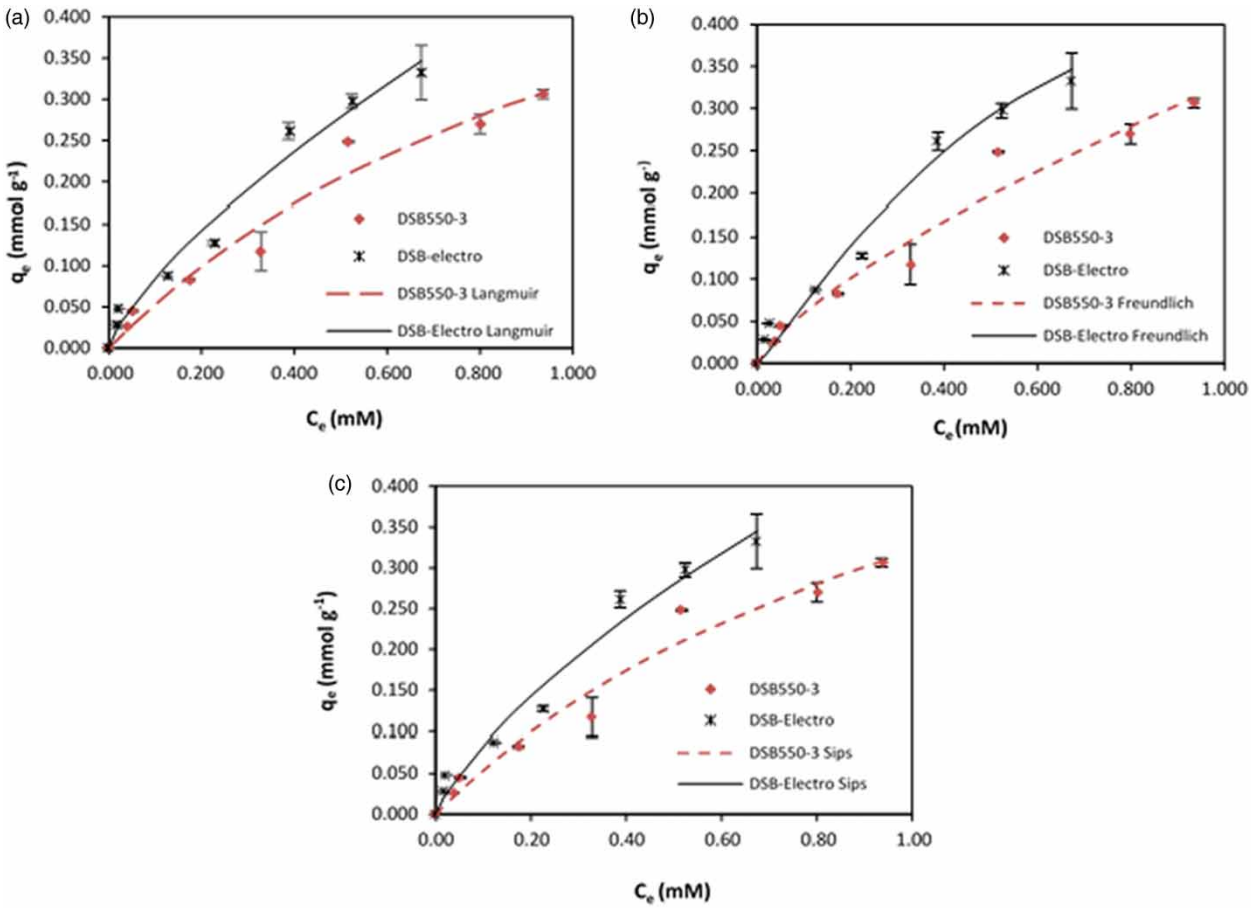

Figure 1 | Electro-assisted adsorption of Pb^{2+} ions onto date seed biochar (biochar: solution = 10 g L^{-1}; C_o = 0.3–4.0 mM; pH = 6; time = 24 h). Symbols represent experimental data. Solid and dashed lines represent isotherm models. (a) Langmuir model; (b) Freundlich model; and (c) Sips model. C_e = metal concentration at equilibrium; DSB-Electro = electro-assisted biochar; q_e = adsorption capacity.

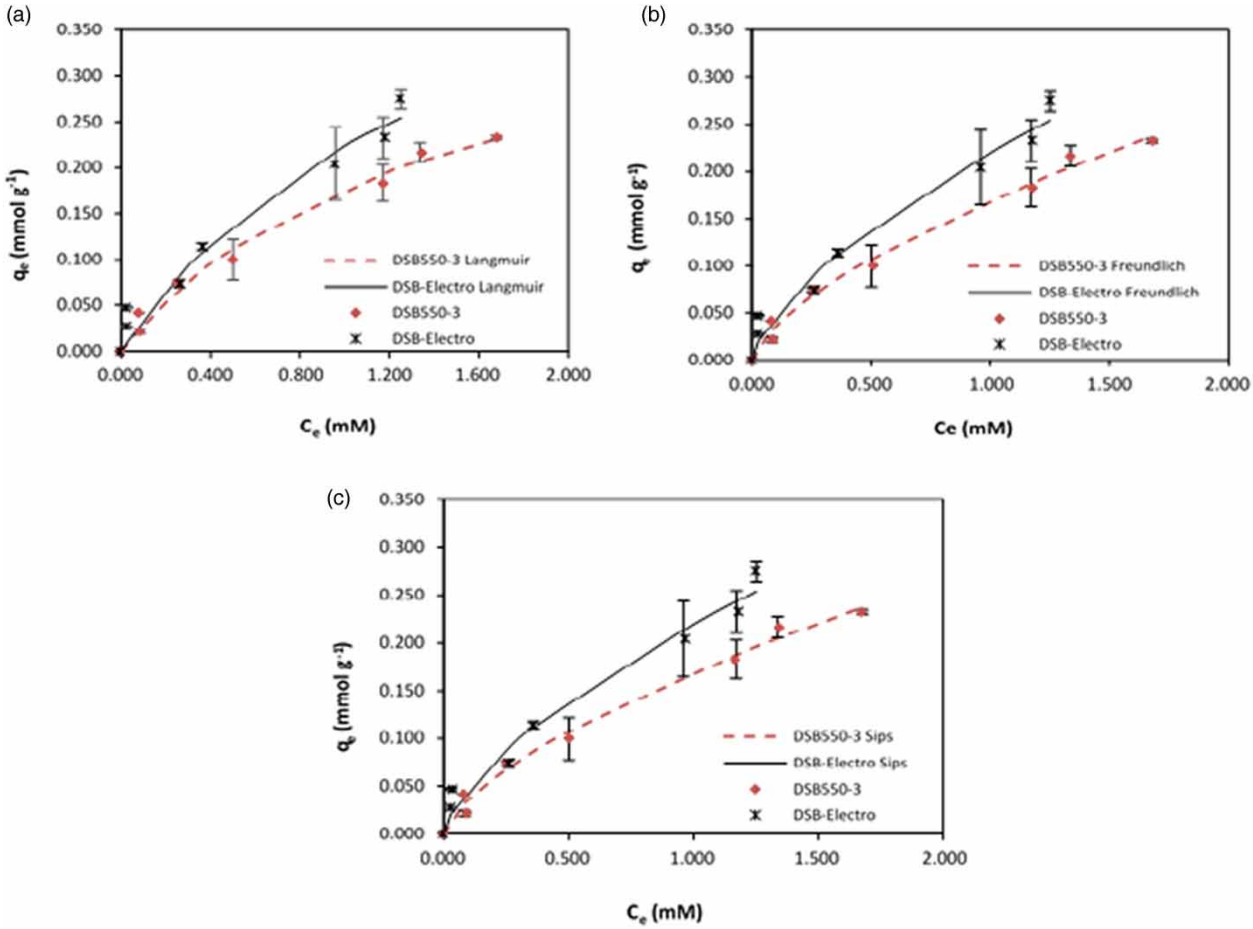

Figure 2 | Electro-assisted adsorption of Cu^{2+} ions onto biochar (biochar: solution = 10 g L^{-1}; C_o = 0.3–4.0 mM; pH = 6; time = 24 h). Symbols represent experimental data. Solid and dashed lines represent isotherm models. (a) Langmuir model; (b) Freundlich model; and (c) Sips model. C_e = metal concentration at equilibrium; DSB-Electro = electro-assisted biochar; q_e = adsorption capacity.

surface under electrical field was mainly due to the high affinity between the surface of adsorbent and adsorbate, which is enhanced by the polarization under electric field.

Significant differences were observed between the adsorption uptake of Pb^{2+} and Cu^{2+} compared with Ni^{2+}. Quantitatively, the adsorption uptake of Ni^{2+} increased (94%) compared with other ions. Several explanations have been proposed to explain this difference. For instance, this could be explained on the basis of their polarizing power. For cations with same charge, the smaller the radius is, the larger the polarizing power is. In our case, soft Lewis acids such as Ni^{2+} show smaller size (0.69 Å) with high polarizing power (2.89) (a large ratio of ionic charge to ionic radius) compared with Cu^{2+} (2.74) and Pb^{2+} (1.67) and consequently, it could form stronger bonds with soft Lewis bases (Reddad *et al.* 2002).

Furthermore, in electrolyte solutions, electricity is conducted by ions travelling between the cathode and anode. The conductivity of the solution depends on the solute and concentration. As such, electrolyte with higher conductivity will have lower resistivity and in turn resistance to movement of the ions. Ohm's law indicates that current is proportionally related to voltage and inversely related to resistance. Therefore, under the same voltage, the solution that has the highest conductivity will involve the movement of more ions (higher current). In our case, the Ni^{2+} solution had the highest electric conductivity (165.12 mS cm^{-1}); thus, it involved more Ni^{2+} ions being transported to the biochar anode giving them greater chance to interact with the surface groups on the biochar. Copper electrolytes have lower conductivity (19.85 mS cm^{-1}) than Ni^{2+} solutions, while lead electrolytes show a conductivity of (24.32 mS cm^{-1}).

Pb^{2+}, Cu^{2+} and Ni^{2+} adsorption onto electro-assisted adsorption biochar was statistically analyzed with the *t*-test and one-way analysis of variance (ANOVA) with a significance level of 0.05 ($p < 0.05$). The results showed

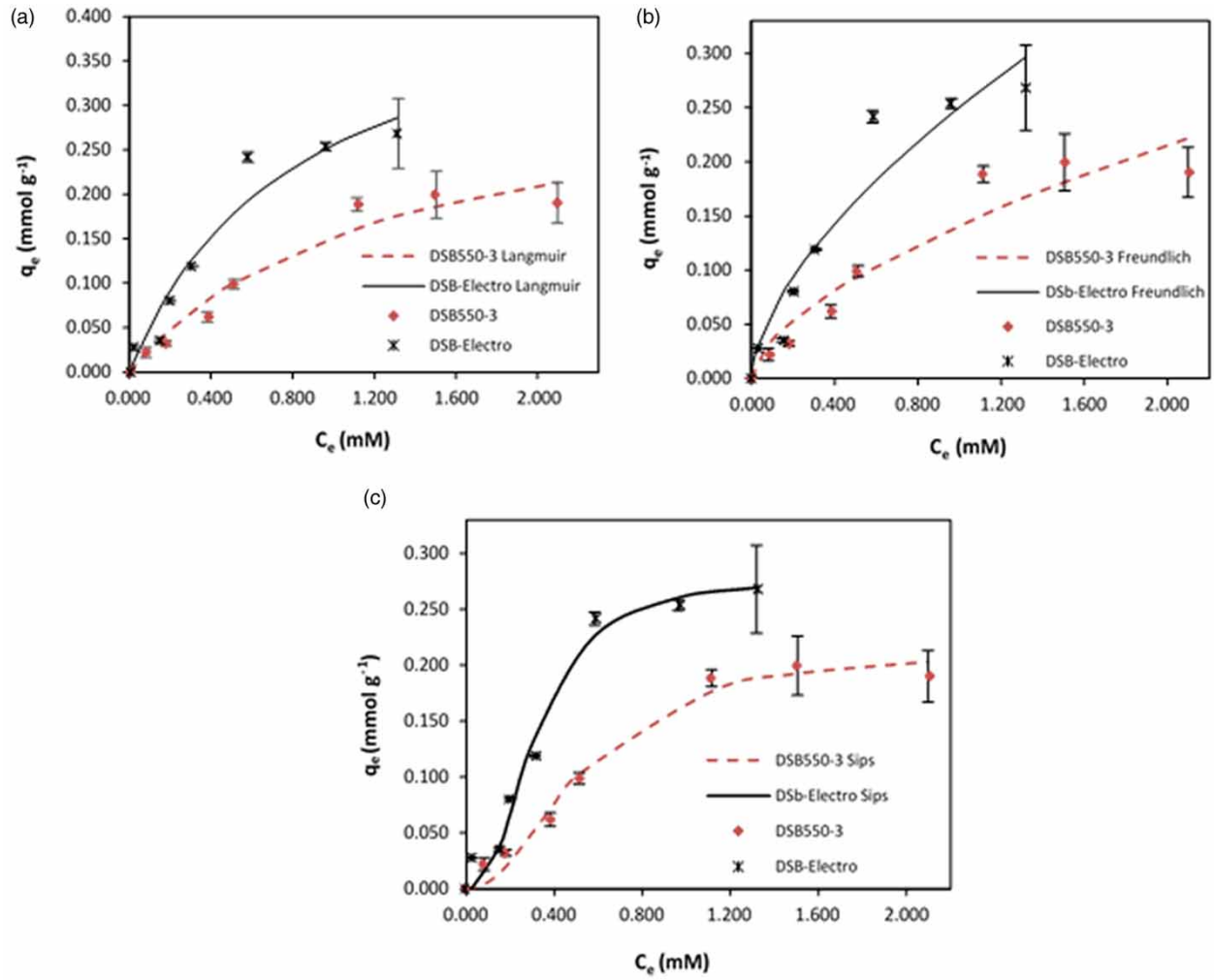

Figure 3 | Electro-assisted adsorption of Ni^{2+} ions onto biochar (biochar: solution = 10 g L^{-1}; C_o = 0.3–4.0 mM; pH = 6; time = 24 h). Symbols represent experimental data. Solid and dashed lines represent isotherm models. (a) Langmuir model; (b) Freundlich model; and (c) Sips model. C_e = metal concentration at equilibrium; DSB-Electro = electro-assisted biochar; q_e = adsorption capacity.

that the maximum adsorption capacities (q_{max}) of Pb^{2+}, Cu^{2+} and Ni^{2+} onto DSB-Electro biochar were statistically and significantly higher than those onto DSB550-3 biochar ($p < 0.05$).

The adsorption isotherms of Pb^{2+}, Cu^{2+} and Ni^{2+} on the electro-assisted biochar were determined using the Langmuir, Sips and Freundlich isotherm models. The experimental results and fitting curves from the three isotherms are shown in Figures 1–3, and the estimated model parameters for the three models are listed in Table 1. The experimental data were better fitted by the Sips isotherm than Langmuir and Freundlich isotherms. The constant K_F ((mmol g^{-1}) (L $mmol^{-1}$)$^{1/n}$) obtained from the Freundlich isotherms for electro-assisted adsorption (0.463, 0.219 and 0.250) were higher than DSB550-3 biochar (0.329, 0.169 and 0.141) for Pb^{2+}, Cu^{2+} and Ni^{2+}, respectively. Furthermore, the adsorption of Pb^{2+}, Cu^{2+} and Ni^{2+} by electro-assisted biochar was favourable in the studied concentration as the adsorption intensity obtained from the Freundlich isotherm (n) was higher than 1.0, suggesting that an effective interaction process occurred between metal ions and the adsorbent (Table 1).

The enhanced adsorption of Pb^{2+}, Cu^{2+} and Ni^{2+} during electro-assisted adsorption could be attributed to the electrostatic interaction. The working principle of electro-adsorption is based on imposing an external electric field in order to force charged species such as metal ions to move toward oppositely charged electrodes (Probstein & Hicks 1993). It was noticed that the solution pH at equilibrium decreased from 6.0 to value of $\approx 5 \pm 0.1$ after Pb^{2+},

Table 1 | Adsorption isotherm parameters for the adsorption of Pb^{2+}, Ni^{2+} and Cu^{2+} ions onto electro-assisted biochar

Isotherm	Pb^{2+}	Cu^{2+}	Ni^{2+}
Langmuir			
K_L (L mmol^{-1})	0.969	0.638	1.226
q_{max} (mmol g^{-1})	0.867	0.572	0.646
R^2	0.990	0.987	0.976
Standard error	0.020	0.011	0.026
Freundlich			
K_F (mmol g^{-1}) (L mmol^{-1})$^{1/n}$	0.463	0.219	0.250
N	1.363	1.513	1.629
R^2	0.987	0.987	0.950
Standard error	0.022	0.018	0.033
Sips			
a_s (L mmol^{-1})	0.234	0.001	16.50
K_s (L g^{-1})	0.555	0.219	4.583
β_s	0.807	0.661	2.446
R^2	0.990	0.992	0.992
Standard error	0.020	0.011	0.011

Cu^{2+} and Ni^{2+} adsorption during the electro-assisted experiments. This could be explained by the release of H^+ from the biochar surface where metal ions are adsorbed, consequently decreasing the solution pH. This phenomenon was also noted by Probstein and Hicks (Probstein & Hicks 1993).

Table 2 shows that electro-assisted adsorption increases the adsorption capacities of biochar. The DSB-Electro biochar produced in this study showed a high adsorption potential for heavy metal ions compared with other modified biochars reported in the literature. For example, our results showed that DSB-Electro biochar exhibited higher adsorption capacity for Pb^{2+}, Cu^{2+} and Ni^{2+} than Hickory biochar treated with NaOH. However, it is hard to compare adsorbents with each other as the adsorption capacity is obtained under specific experimental conditions including type of modification method, method of preparation, solution pH, temperature, initial metal concentration, and particle size.

Adsorption kinetics

Figures 4–6 show the time profiles of the adsorbed amount of Pb^{2+}, Cu^{2+} and Ni^{2+} as a function of contact time. As clearly presented, the metal ions adsorption onto electrode occurred rapidly; for example, around 88% of Pb^{2+} and Ni^{2+} ions adsorbed within the first 3 h, while 96% of total adsorption of Cu^{2+} ion occurred at the first hour contact time. The fast adsorption at initial stage can be attributed to rapid external mass transfer and surface adsorption associated with the availability of large number of vacant surface sites for adsorption. Thus, the amount of adsorbate accumulated on the biochar surface rapidly increases. However, the subsequent gradual adsorption is due to the rate-limited intraparticle diffusion associated with fewer metal ions that accumulated onto the adsorption sites.

The adsorption kinetic data were determined using pseudo first order and pseudo second order models. Pseudo second order model gives a better fit ($R^2 \geq 0.93$) for Pb^{2+}, Cu^{2+} and Ni^{2+} than pseudo first order model (Table 3). Furthermore, the calculated q_{calc} value (mmol g^{-1}) obtained from pseudo second order was considerably close to the experimental q_{exp} value (mmol g^{-1}) as seen in

Table 2 | Adsorption capacity of unmodified and modified biochars for heavy metal removal. DSB-Electro = electro-assisted biochar

Biochar	Pyrolysis temperature (°C)	pH	Ion	q_{max} (mmol g^{-1})	References
Hickory treated with NaOH	600	5.0	Pb^{2+}	0.092	Ding *et al.* (2016)
			Cu^{2+}	0.281	
			Ni^{2+}	0.015	
Peanut hull treated with H_2O_2	300	–	Pb^{2+}	0.110	Xue *et al.* (2012)
Corn straw treated with MnOx	600	6.0	Cu^{2+}	0.291–2.526	Song *et al.* (2014)
Switchgrass treated with KOH	300	5.0	Cu^{2+}	0.487	Regmi *et al.* (2012)
Date seed biochar	550	6.0	Pb^{2+}	0.718	This study
			Cu^{2+}	0.421	
			Ni^{2+}	0.333	
DSB-Electro			Pb^{2+}	0.867	
			Cu^{2+}	0.572	
			Ni^{2+}	0.646	

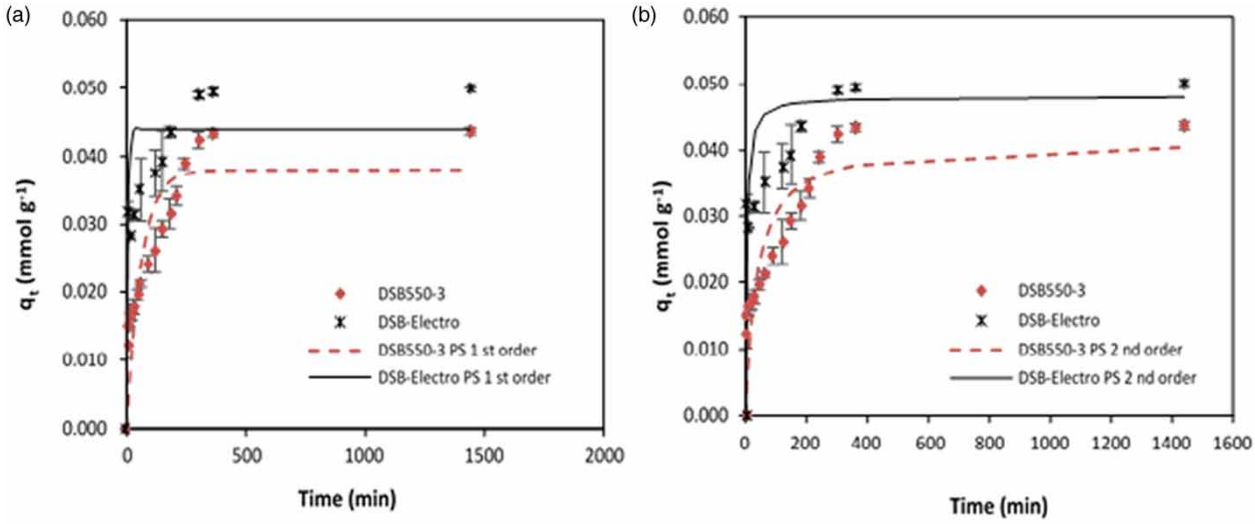

Figure 4 | Electro-assisted adsorption kinetics of Pb^{2+} ions. Symbols represent experimental data, while lines represent (a) pseudo (PS) first order, (b) pseudo second order. DSB-Electro = electro-assisted biochar; q_t = amount of metal ion adsorbed per unit mass at time t.

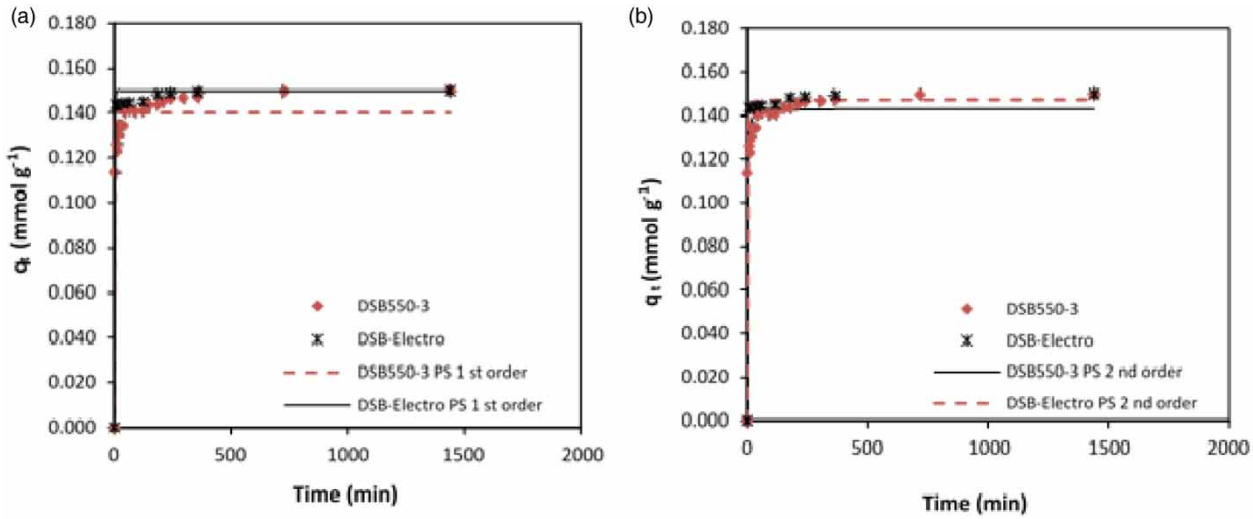

Figure 5 | Electro-assisted adsorption kinetics of Cu^{2+} ions. Symbols represent experimental data, while lines represent (a) pseudo (PS) first order, (b) pseudo second order. DSB-Electro = electro-assisted biochar; q_t = amount of metal ion adsorbed per unit mass at time t.

Table 3. Pseudo second order model also confirms the observed behaviour of faster adsorption as the parameter k_2, adsorption rate constant, for the DSB-Electro biochar (5.733, 33.78 and 7.098 g mmol^{-1} min^{-1}) is much higher than for DSB550-3 (0.676, 10.35 and 0.232 g mmol^{-1} min^{-1}) for Pb^{2+}, Cu^{2+} and Ni^{2+}, implying faster adsorption rate. Haro *et al.* (2011) reported that the fast-electro-assisted ion adsorption kinetics of the carbon-based electrode might be due to the combination of an interconnected micro/mesoporous matrix. Faster adsorption rate might be also due to the increased concentration of metal ions near the anode, which increases the drive force for diffusion.

Spectroscopy analysis of electro-assisted biochar surface

Scanning electron microscope (SEM) images of DSB550-3 before electro-assisted and after electro-assisted metal ion adsorption were analysed. As can be seen from Figure 7,

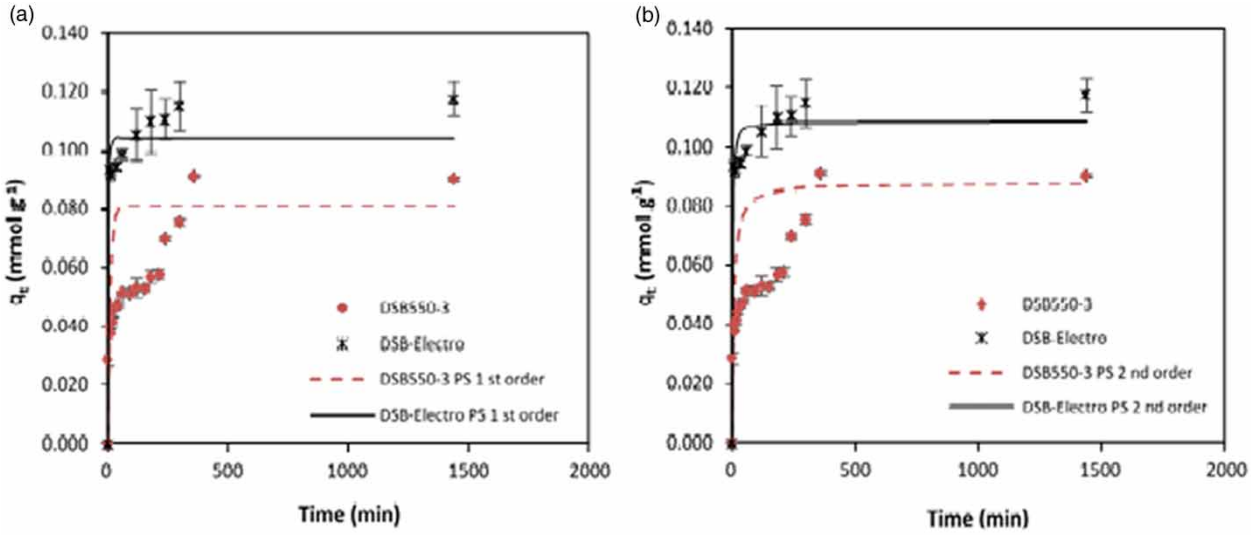

Figure 6 | Electro-assisted adsorption kinetics of Ni^{2+} ions. Symbols represent experimental data, while lines represent (a) pseudo (PS) first order, (b) pseudo second order. DSB-Electro = electro-assisted biochar; q_t = amount of metal ion adsorbed per unit mass at time t.

Table 3 | Kinetics parameters of heavy metal removal onto electro-assisted biochar

Model	Pb^{2+}	Cu^{2+}	Ni^{2+}
Pseudo first order model			
q_{exp} (mmol g^{-1})	0.050	0.148	0.177
q_{calc} (mmol g^{-1})	0.042	0.149	0.104
k_1 (min^{-1})	0.194	0.717	2.871
R^2	0.900	0.980	0.960
Standard error	0.007	0.002	0.010
Pseudo second order model			
q_{exp} (mmol g^{-1})	0.050	0.148	0.117
q_{calc} (mmol g^{-1})	0.044	0.149	0.109
k_2 (g mmol^{-1} min^{-1})	5.773	33.78	7.098
R^2	0.930	1.000	0.980
Standard error	0.006	0.002	0.006

the SEM image of the DSB550-3 biochar (non-electro assisted) (Figure 7(a)) shows less apparent pores on the surface in comparison with the DSB-Electro one (after electro-adsorption) (Figure 7(b)–7(d)). The surface morphological structure of DSB-Electro biochar showed a rough and porous structure which can provide channels for the adsorbates to reach the active adsorption sites and promote the rapid adsorption to reach equilibrium faster. The increase in pore structure might be attributed to the effect of the electric current which caused some of the negatively charged impurities to repel thus opening the pores which were blocked by the impurities (ash and minerals). SEM images confirm that biochar electrode is highly porous material and thus physical adsorption is considered as one of the mechanisms responsible for heavy metal adsorption onto the biochar electrode (Haro *et al.* 2011). This can be seen in images after adsorption (Figure 7(b)–7(d) SEM) which show the pores of biochar packed with metal ions.

The enhanced adsorption of Pb^{2+}, Cu^{2+} and Ni^{2+} during electro-assisted adsorption can be also related to the surface functional groups presented onto biochar surface as indicated by the Fourier transform infrared spectroscopy spectra (Figure 8). The spectral analysis of the DSB-Electro biochar after Pb^{2+} adsorption (Figure 8) shows various surface functional groups. For instance, significant differences at the peaks 2,325, 2,652.37 and 1,979.97 were observed for both biochars after Pb^{2+} adsorption, confirming that functional groups such as C ≡ C, O–H and C = O participated in binding ions onto the biochar. The peaks at 1,564.4, 1,127 and 1,070.83 cm^{-1} in both biochars after Pb^{2+} adsorption were also observed, confirming that functional groups such as C–O, N–O, O-H and COO− groups were involved in binding ions onto the biochar.

Desorption of electro-assisted laden biochar

In order to investigate the potential reversibility of electro-assisted biochar (i.e. desorption) for the metal ions retained at the electrode under an external electric field, adsorption–desorption reversibility of the electrode was investigated by reversing the external electric field. First, the

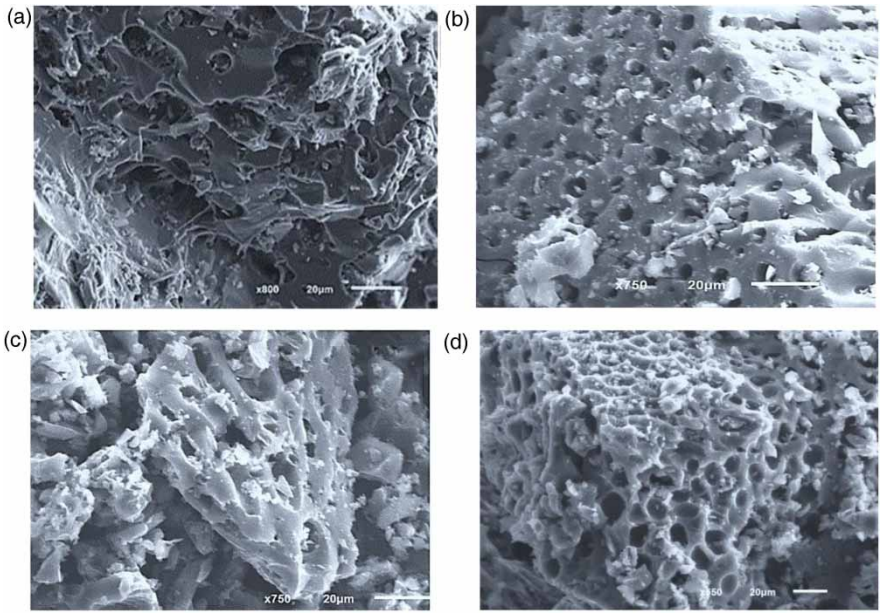

Figure 7 | Scanning electron microscope images of biochar before adsorption (non-electro) and after (DSB-Electro) (a) before adsorption (DSB550-3); (b) after Cu^{2+} adsorption; (c) after Ni^{2+} adsorption; (d) after Pb^{2+} adsorption.

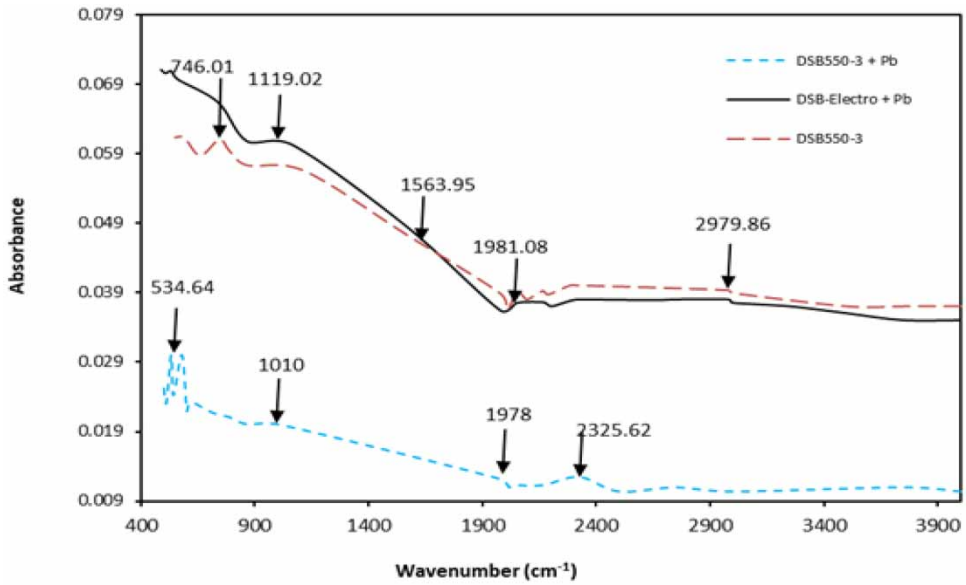

Figure 8 | Fourier transform infrared spectroscopy spectra of before and after Pb^{2+} adsorption onto DSB550-3 biochar and electro-assisted biochar (DSB-Electro).

electro-assisted adsorption experiment was conducted by setting the biochar electrode as the anode as described earlier. After 24 h the electric field was disconnected, and samples were obtained to determine the amount of metals adsorbed on the biochar. Second, the electric field was reversed by reversing the polarity (setting the biochar electrode as the cathode) for 24 h. Finally, samples were collected to determine the amount of metals released to the solution. Reversing the polarity did not seem to cause significant desorption of the adsorbed metals from the biochar. The amount released from reversing polarity of Pb^{2+}, Cu^{2+} and Ni^{2+} was 28.5%, 37% and 34%, respectively.

As the electro-assisted adsorption process relies on electrostatic attraction, it would be expected that the process could be fully reversible (Haro *et al.* 2011). However, the experimental results showed that a fraction of the metal ions is not leached out upon the reversing of the polarization and remained inside the porous structure of the biochar electrode. This indicates that only a fraction of the ions was held by the electrostatic charge introduced by the current. It is likely that the enhanced charge facilitated other adsorption mechanisms by bringing the ions in contact with biochar initially via electrostatic force. Additionally, as electrical potential is only playing an 'assistant' role and is only one of the aspects in the adsorption process, we probably cannot expect a full recovery; rather the extra amount adsorbed may be fully recoverable by reversing the polarity.

CONCLUSION

For any adsorption system, the adsorption rate and capacity are two important factors affecting the performance of the process. This work investigates electro-adsorption of Pb^{2+}, Cu^{2+} and Ni^{2+} from aqueous solutions by biochar. Biochar has been introduced to be an ideal material for an electrode because of its low electrical resistivity and its porous structure with high surface area. The results confirmed that electro-assisted adsorption enhanced the adsorption rate as well as capacity of biochar for heavy metals. The adsorption capacity of DSB-Electro biochar increased by 21%, 36% and 94% for Pb^{2+}, Cu^{2+} and Ni^{2+}, respectively. Metal ion adsorption onto electrode occurred rapidly; for example, around 88% of Pb^{2+} and Ni^{2+} adsorbed within the first 3 h, while 96% of total adsorption of Cu^{2+} occurred within the first hour of contact. The enhanced adsorption of aqueous Pb^{2+}, Cu^{2+} and Ni^{2+} during electro-assisted adsorption can be attributed to bringing the ions into closer contact with the biochar and increasing the surface charge density on the surface of the biochar which were subsequently held by other mechanisms such as electrostatic interaction, surface complexation, and physical surface adsorption. Electro-assisted adsorption can improve the biochar economic feasibility for metals removal (particularly Ni^{2+}) from industrial streams by increasing the capacity and reducing the quantities of waste. It is further recommended to investigate the cost-effectiveness of electro-assisted biochar application as well as the reusability of biochar from a life-cycle perspective.

CREDIT AUTHOR STATEMENT

Zainab Mahdi: Writing – original draft preparation; writing – editing and revision; conceptualization; methods; software; investigation; data analysis; data curation.

Ali El Hanandeh: Writing – original draft preparation; writing – editing and revision; conceptualization; supervision, resources.

Qiming Jimmy Yu: Writing – editing and revision; supervision; resources.

SUPPLEMENTARY MATERIAL

The Supplementary Material for this paper is available online at https://dx.doi.org/10.2166/wst.2020.163.

REFERENCES

Ahmad, T., Rafatullah, M., Ghazali, A., Sulaiman, O. & Hashim, R. 2011 Oil palm biomass–based adsorbents for the removal of water pollutants – a review. *Journal of Environmental Science and Health, Part C* **29**, 177–222.

Ahmad, M., Lee, S. S., Dou, X., Mohan, D., Sung, J. K., Yang, J. E. & Ok, Y. S. 2012 Effects of pyrolysis temperature on soybean stover- and peanut shell-derived biochar properties and TCE adsorption in water. *Bioresource Technology* **118**, 536–544.

Chen, B., Chen, Z. & Lv, S. 2011 A novel magnetic biochar efficiently sorbs organic pollutants and phosphate. *Bioresource Technology* **102**, 716–723.

Ding, Z., Hu, X., Wan, Y., Wang, S. & Gao, B. 2016 Removal of lead, copper, cadmium, zinc, and nickel from aqueous solutions by alkali-modified biochar: batch and column tests. *Journal of Industrial and Engineering Chemistry* **33**, 239–245.

Grimm, J., Bessarabov, D. & Sanderson, R. 1998 Review of electro-assisted methods for water purification. *Desalination* **115**, 285–294.

Han, Y., Quan, X., Chen, S., Zhao, H., Cui, C. & Zhao, Y. 2006 Electrochemically enhanced adsorption of phenol on activated carbon fibers in basic aqueous solution. *Journal of Colloid and Interface Science* **299**, 766–771.

Haro, M., Rasines, G., Macias, C. & Ania, C. O. 2011 Stability of a carbon gel electrode when used for the electro-assisted removal of ions from brackish water. *Carbon* **49**, 3723–3730.

Jung, K.-W., Jeong, T.-U., Hwang, M.-J., Kim, K. & Ahn, K.-H. 2015 Phosphate adsorption ability of biochar/Mg–Al assembled nanocomposites prepared by aluminum-electrode based electro-assisted modification method with MgCl2 as electrolyte. *Bioresource Technology* **198**, 603–610.

Kaewsarn, P. 2000 *Single and Multi-Component Biosorption of Heavy Metal Ions by Biosorbents From Marine Alga*

Durvillaea Potatarum. *Doctor of Philosophy*, Griffith University.

Mahdi, Z., El Hanandeh, A. & Yu, Q. J. 2019 Preparation, characterization and application of surface modified biochar from date seed for improved lead, copper, and nickel removal from aqueous solutions. *Journal of Environmental Chemical Engineering* **7**, 103379.

Mohan, D., Sarswat, A., Ok, Y. S. & Pittman, C. U. 2014 Organic and inorganic contaminants removal from water with biochar, a renewable, low cost and sustainable adsorbent – a critical review. *Bioresource Technology* **160**, 191–202.

Pirkarami, A., Olya, M. E. & Yousefi Limaee, N. 2013 Decolorization of azo dyes by photo electro adsorption process using polyaniline coated electrode. *Progress in Organic Coatings* **76**, 682–688.

Probstein, R. F. & Hicks, R. E. 1993 Removal of contaminants from soils by electric fields. *Science* **260**, 498–503.

Rajapaksha, A. U., Chen, S. S., Tsang, D. C. W., Zhang, M., Vithanage, M., Mandal, S., Gao, B., Bolan, N. S. & Ok, Y. S. 2016 Engineered/designer biochar for contaminant removal/immobilization from soil and water: potential and implication of biochar modification. *Chemosphere* **148**, 276–291.

Reddad, Z., Gerente, C., Andres, Y. & Le Cloirec, P. 2002 Adsorption of several metal ions onto a low-cost biosorbent: kinetic and equilibrium studies. *Environmental Science & Technology* **36**, 2067–2073.

Regmi, P., Garcia Moscoso, J. L., Kumar, S., Cao, X., Mao, J. & Schafran, G. 2012 Removal of copper and cadmium from aqueous solution using switchgrass biochar produced via hydrothermal carbonization process. *Journal of Environmental Management* **109**, 61–69.

Sarkar, A., Ranjan, A. & Paul, B. 2019 Synthesis, characterization and application of surface-modified biochar synthesized from rice husk, an agro-industrial waste for the removal of hexavalent chromium from drinking water at near-neutral pH. *Clean Technologies and Environmental Policy* **21**, 447–462.

Song, Z., Lian, F., Yu, Z., Zhu, L., Xing, B. & Qiu, W. 2014 Synthesis and characterization of a novel MnOx-loaded biochar and its adsorption properties for Cu^{2+} in aqueous solution. *Chemical Engineering Journal* **242**, 36–42.

Stephanie, H. 2017 *Using Biochar Electrodes for Brackish Water Desalination*. 10606138 M.S., Mississippi State University.

Usman, A. R. A., Abduljabbar, A., Vithanage, M., Ok, Y. S., Ahmad, M., Ahmad, M., Elfaki, J., Abdulazeem, S. S. & Al-Wabel, M. I. 2015 Biochar production from date palm waste: charring temperature induced changes in composition and surface chemistry. *Journal of Analytical and Applied Pyrolysis* **115**, 392–400.

Wu, W., Li, J., Lan, T., Müller, K., Niazi, N. K., Chen, X., Xu, S., Zheng, L., Chu, Y. & Li, J. 2017 Unraveling sorption of lead in aqueous solutions by chemically modified biochar derived from coconut fiber: a microscopic and spectroscopic investigation. *Science of the Total Environment* **576**, 766–774.

Xue, Y., Gao, B., Yao, Y., Inyang, M., Zhang, M., Zimmerman, A. R. & Ro, K. S. 2012 Hydrogen peroxide modification enhances the ability of biochar (hydrochar) produced from hydrothermal carbonization of peanut hull to remove aqueous heavy metals: batch and column tests. *Chemical Engineering Journal* **200–202**, 673–680.

Ying, T.-Y., Yang, K.-L., Yiacoumi, S. & Tsouris, C. 2002 Electrosorption of ions from aqueous solutions by nanostructured carbon aerogel. *Journal of Colloid and Interface Science* **250**, 18–27.

Zou, L., Morris, G. & Qi, D. 2008 Using activated carbon electrode in electrosorptive deionisation of brackish water. *Desalination* **225**, 329–340.

First received 5 January 2020; accepted in revised form 26 March 2020. Available online 7 April 2020